# SC42056: Non-Linear Optimization Assignment

Alexandra Ministeru, Weihong Tang

October 25, 2021

## 1 Introduction

This assignment employs non-linear optimization methods to minimize power consumption of a Heating, Ventilation and Air-Conditioning (HVAC) system by identifying optimal values of two control parameters. The last three digits of the student numbers are 432 and 160 respectively, such that $E_1$, $E_2$ and $E_3$ parameters have the following values:

$$E_1 = 5, E_2 = 9, E_3 = 2$$

## 2 Discrete time state-space model

The state of the system consists of four temperatures: $T_a$ - indoor air temperature, $T_{w,1}$ - temperature of the vertical glass facades, $T_{w,2}$ - temperature of the ceiling, $T_{w,3}$ - temperature of the floor. These temperatures depend on the previous state, the ventilation factor $u(k)$ and shading factor $v(k)$ through a non-linear mapping function. The energy required by the backup system is the output of the state-space model, which also depends in a non-linear manner on the previous state, $u(k)$ and $v(k)$. The state vector $X$ can be written as in relation 1.

$$x(k) = \begin{bmatrix} x_1(k) \\ x_2(k) \\ x_3(k) \\ x_4(k) \end{bmatrix} = \begin{bmatrix} T_a(k) \\ T_{w,1}(k) \\ T_{w,2}(k) \\ T_{w,3}(k) \end{bmatrix} \tag{1}$$

According to the relations given in the assignment, the discrete-time state-space model is:

$$\begin{cases} x(k+1) = f(x(k), u(k), v(k)) = [x_1(k+1) \quad x_2(k+1) \quad x_3(k+1) \quad x_4(k+1)]^T \\ y(k) = g(x(k), u(k)) \end{cases}, \tag{2}$$

where

$$\begin{aligned} x_1(k+1) &= x_1(k) + [\dot{q}_p(k) + \dot{m}(k) C_a [T_0(k) - x_1(k)] + h_a A_1 [x_2(k) - x_1(k)] \\ &\quad + h_a A_2 [x_3(k) - x_1(k)] + haA_3 [x_4(k) - x_1(k)] \frac{\Delta t}{\rho_a V_a c_a} \\ x_2(k+1) &= x_2(k) + \left[ v(k) I(k) \alpha_{w,1} + \lambda \left[ T_{sky}^4(k) - x_2^4(k) \right] + h_0 [T_0(k) - x_2(k)] \right. \\ &\quad \left. + h_a [x_2(k) - x_1(k)] \right] \frac{A_{w,1} \Delta t}{\rho_{w,1} V_{w,1} C_{w,1}} \\ x_3(k+1) &= x_3(k) + \left[ I(k) \alpha_{w,2} + \lambda \left[ T_{sky}^4(k) - x_3^4(k) \right] + h_0 [T_0(k) - x_3(k)] \right. \\ &\quad \left. + h_a [x_3(k) - x_1(k)] \right] \frac{A_{w,2} \Delta t}{\rho_{w,2} V_{w,2} C_{w,2}} \\ x_4(k+1) &= x_4(k) + [0.5 v(k) I(k) \tau_{w,1} \alpha_{w,2} + h_a [x_4(k) - x_1(k)]] \frac{A_{w,3} \Delta t}{\rho_{w,3} V_{w,3} C_{w,3}} \end{aligned} \tag{3}$$

The output of the state-space model is given by:

$$g(x(k), u(k)) = q_{\text{backup}}\ (k) = \dot{m}(k) C_a \left| x_1(k) - T_{\text{ref}} \right| \Delta t + \beta \left[ x_1(k) - T_{\text{ref}} \right]^2 \tag{4}$$

The initial state is illustrated in relation 5.

$$x(0) = \begin{bmatrix} x_1(0) \\ x_2(0) \\ x_3(0) \\ x_4(0) \end{bmatrix} = \begin{bmatrix} T_a(0) \\ T_{w,1}(0) \\ T_{w,2}(0) \\ T_{w,3}(0) \end{bmatrix} = \begin{bmatrix} 16°\text{C} \\ 16°\text{C} \\ 16°\text{C} \\ 16°\text{C} \end{bmatrix} \tag{5}$$

The air mass flow rate is given by the following equation:

$$\dot{m}(k) \quad = \rho_{\mathrm{a}} u(k) \phi \sqrt{2gH \max\left[0, \frac{T_{\mathrm{a}}(k) - T_{\mathrm{o}}(k)}{T_{\mathrm{a}}(k)}\right]} \tag{6}$$

Based on the group's specific parameters $E_1, E_2$ and $E_3$, the solar incidence, outside temperature, and heat rate from occupancy are as follows:

$$I(k) \quad = \begin{cases} 300 + 5 \text{ W/m}^2 & \text{if } k < 48 \\ 700 + 5 \text{ W/m}^2 & \text{if } 48 \leq k \leq 96 \\ 300 + 5 \text{ W/m}^2 & \text{if } k > 96 \end{cases}$$

$$T_{\mathrm{o}}(k) \quad = \begin{cases} 12 + 0.9°\text{C} & \text{if } k < 48 \\ 18 + 0.9°\text{C} & \text{if } 48 \leq k \leq 96 \\ 17 + 0.9°\text{C} & \text{if } k > 96 \end{cases}$$

$$\dot{q}_{\mathrm{p}}(k) \quad = \begin{cases} 5000 + 20 \text{ W} & \text{if } k < 48 \\ 25000 + 20 \text{ W} & \text{if } 48 \leq k \leq 96 \\ 20000 + 20 \text{ W} & \text{if } k > 96 \end{cases}$$

The values of the system properties (including four segments: Air, Facade, Ceiling and Floor) are shown in Table 1. Besides, other constant parameters include penalization factor $\beta = 10^6 K^{-2}$, $\Delta t = 5min$, reference temperature $T_{ref} = 21°\text{C}$, the sky temperature $T_{sky}(k) = T_o(k) - 8°\text{C}$, the tower height $H = 5m$, the cross-flow area $\phi = 3m^2$, the heat transfer coefficients $h_a = 5\frac{W}{m^2 K}$, $h_0 = 25\frac{W}{m^2 K}$ and $\lambda = 4.5 \cdot 10^{-8} \frac{W}{m^2 K^4}$.

| Segment | Subscript | $V\left[\text{ m}^3\right]$ | $A\left[\text{ m}^2\right]$ | $C\left[\frac{\text{J}}{\text{kgK}}\right]$ | $\rho\left[\frac{\text{kg}}{\text{m}^3}\right]$ | $\alpha[-]$ | $\tau[-]$ |
|---|---|---|---|---|---|---|---|
| Air | a | 1430 | - | 1005 | 1.2 | - | - |
| Facade | w, 1 | 17.5 | 350 | 900 | 2500 | 0.085 | 0.9 |
| Ceiling | w, 2 | 15 | 286 | 840 | 2000 | 0.2 | - |
| Floor | w, 3 | 80 | 286 | 840 | 2000 | 0.6 | - |

Table 1: System properties, reproduced from the original assignment paper

# 3 Formulated optimization problem

The total energy demanded by the auxiliary backup system over a 12-hour time span can be obtained by summing the value of the energy $q_{backup}(k)$ at each time step $k$. This becomes the objective function that must be minimized with regard to $u(k)$ and $v(k)$.

$$\min_{\substack{u(0),\ldots,u(144) \\ v(0),\ldots,v(142)}} \sum_{k=0}^{144} q_{backup}(k) \tag{7}$$

Additionally, fractions $u(k)$ and $v(k)$ must range between 0 and 1, therefore the optimization problem has the inequality constraints shown in 8.

$$\begin{aligned} 0 \leq u(k) \leq 1 \\ 0 \leq v(k) \leq 1 \\ k = 1, \ldots, 144 \end{aligned} \tag{8}$$

# 4 Optimization algorithm

The optimization problem illustrated in equation 7 is a nonlinear, nonconvex problem, since an absolute value function, a square root term and terms such as $T_{w,1}^4(k)$, $T_{w,3}^4(k)$ and $T_a^2(k)$ appear in the expression of $q_{backup}(k)$. Given that constraints are specified for the objective function variables

$u(k)$ and $v(k)$, it is necessary to select an algorithm appropriate for nonlinear, nonconvex optimization with (linear inequality) constraints. For this purpose, the MATLAB *fmincon* function was chosen.

The function *fmincon* has as available solving algorithms SQP and Interior-Point. In order for the algorithms to converge to a solution, the implicit number of maximum iterations and function evaluations was increased. SQP algorithm converged to a solution with significantly less iterations and function evaluations compared to Interior Point. Besides, Interior Point is generally used to solve convex problems. Therefore, SQP is the algorithm used throughout the following sections.

The objective function passed as a parameter to *fmincon* computes the state and the value of the required backup energy at each time step $k$. It depends on fractions $u$ and $v$, which are stacked in a single argument vector.

# 5 Starting points comparison

Firstly, the optimization algorithm was given a 0.1 initial condition for all control factors. A solution was found after 242 iterations. At this optimum point, the objective function has the value $fval_1 \approx 1.3638e+09$.

As a second starting point, the initial condition vector had a value of 0.9 on all positions. There were 196 necessary iterations for the algorithm to identify a solution, with $fval_2 \approx 1.3638e+09$ (resembling the previous value, figure 2b). A visual comparison between the two solutions is illustrated in figures 1a and 1b.

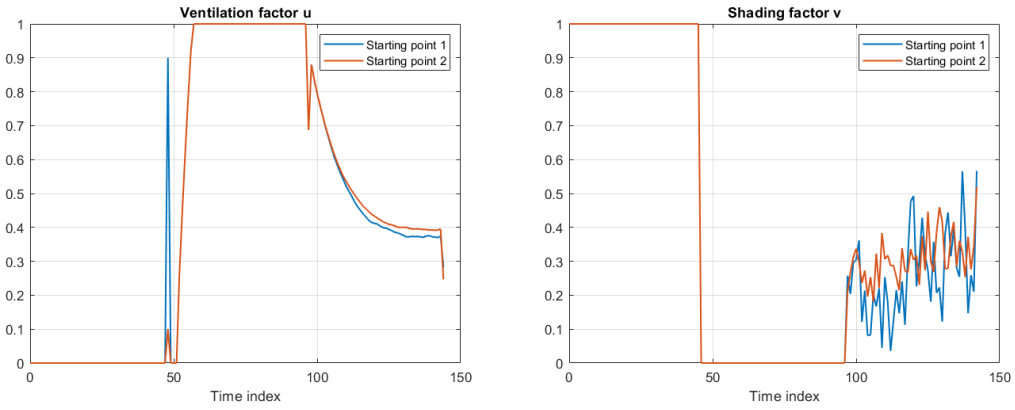


(a) Ventilation factor $u$

(b) Shading factor $v$

Figure 1: Comparison of optimization problem solutions for two different starting points.

The two solutions have a similar evolution. In both cases, ventilation factor $u$ is constant and equal to zero for the first 4 hours ($k < 48$). As a consequence, during this period the energy demand reaches its highest value (shown in figure 2a), due to the difference between the indoor and reference temperature amplified by the penalization factor. After the outdoor temperature becomes greater than the indoor temperature at $k = 48$, the ventilation factor increases to the maximum value, which results in a decrease of backup energy demand. During the last time interval, the computed $u$ decreases as $T_a$ has reached $T_{ref}$ (illustrated in figure 3).

Shading factor $v$ has a similar evolution during the first 8 hours ($k < 96$). After 4 hours, it is set to minimum value 0, such that the increased solar incidence does not affect the energy demand. After 8 hours, more significant differences between the two solutions can be observed in shading factor $v$. During this time interval, $T_a$ is kept at the $T_{ref}$ level through $v$ and, thus, the energy demand decreases to an almost zero value.

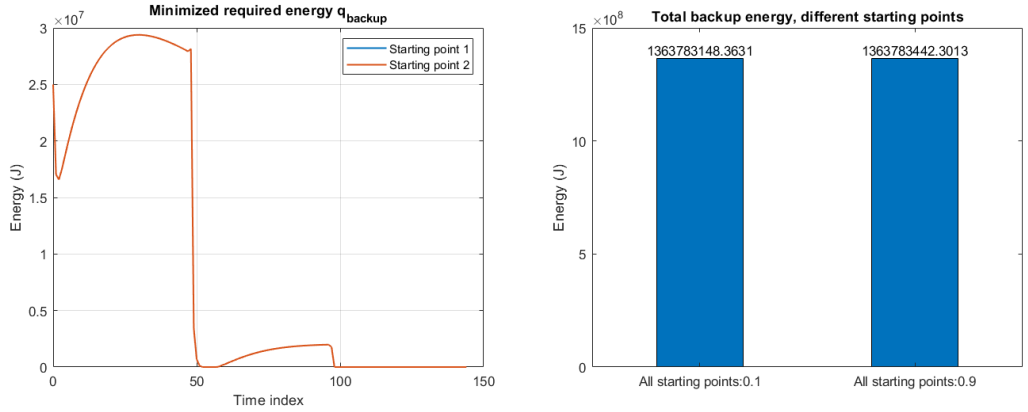


(a) Required backup energy along time interval (b) Objective function values

Figure 2: Backup energy comparison

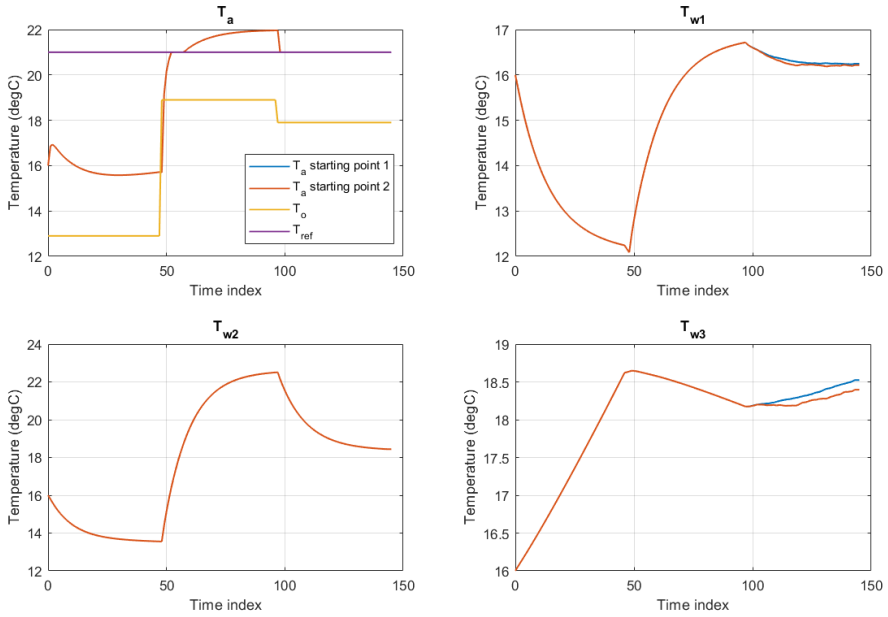


Figure 3: Comparison of state evolution

# 6 Global optimum

Solving the optimization problem using the SQP algorithm does not guarantee that the global optimum was reached, since the solution might also correspond to a local optimum point. The solution depends on the starting point provided to the algorithm and how it is positioned with respect to the global optimum.

Investigating specific global optimization techniques (such as multi-start local optimization) and algorithms (genetic algorithms, simulated annealing) can lead to an improved solution [vdBS21]. Figures 4a and 4b provide a comparison between solutions identified with the three enumerated methods. Multi-start local optimization was performed on six different equally distanced starting points. The solution provided by the genetic algorithm resembles those obtained using the SQP algortihm for the first 8 hours ($k < 98$) and has greater variation over the last time subinterval. Simulated annealing lead to a solution with numerous variations across the time horizon.

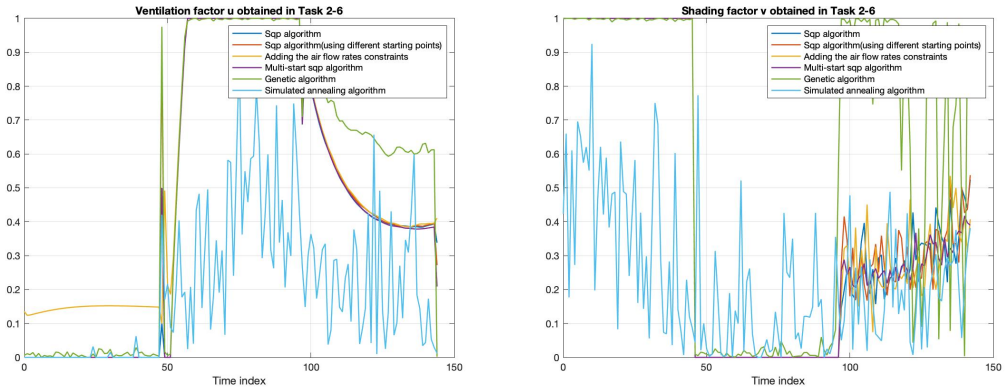


(a) Ventilation factor $u$ (b) Shading factor $v$

Figure 4: Solution comparison

Figure 5a illustrates the total backup energy obtained using the global optimization methods. Multi-start local optimization and the genetic algorithm lead an approximately similar value of the objective function, with the genetic algorithm evaluation being slightly higher. Employing simulated annealing resulted in a significantly larger amount of energy required. Therefore, this algorithm is not appropriate for the current purpose. Since SQP minimization, SQP multi-start local minimization and the genetic algorithm lead to similar solutions and results, it can be concluded that the global optimum was found.

Additionally, it must be taken into consideration that global optimization is significantly more time consuming, as illustrated in figure 5b. Simulated annealing required the largest amount of time, approximatively 33 times longer than SQP local minimization for the displayed program run. It was followed by the genetic algorithm and the multi-start SQP minimization. Therefore, in this particular context, running the SQP algorithm once is enough to identify a satisfactory solution.

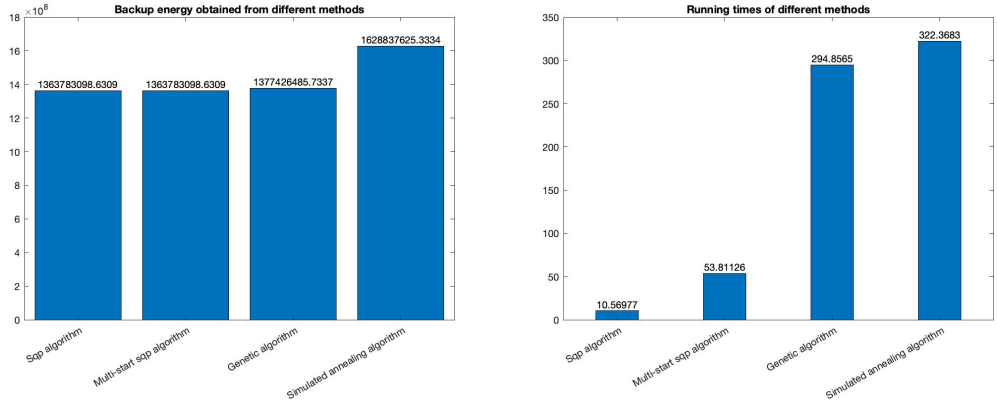


(a) Total backup energy $q_{backup}$ (b) Running time

Figure 5: Global optimization comparison

# 7 Air flow constraint

In order to limit the minimum air flow $\dot{m}$ to 0.5 kg/s, a nonlinear constraint is defined for each time step $k$, as illustrated in equation 9.

$$-\dot{m}(k) + 0.5 < 0,\ k = 1, \ldots, 144 \tag{9}$$

In figure 6a it can be observed that the ventilation factor $u$ has non-zero values during the first 48 time samples, as opposed to the previous case. This is caused by the air mass flow constraint, since a

zero value of $u(k)$ would render $\dot{m}(k)$ to have a zero value. Shading factor $v$ has a similar evolution to the previous cases. The objective function is evaluated to $fval_{ncon} \approx 1.5347e+09$.

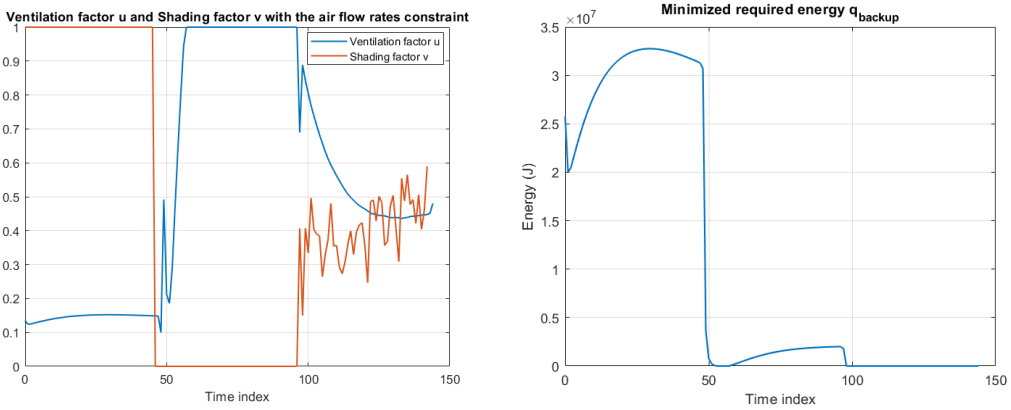


(a) Solution, fractions $u$ and $v$

(b) Demanded energy $q_{backup}$

Figure 6: Solution of optimization algorithm with air flow constraint

The evolution of the constrained air mass flow is illustrated in figure 7a. The solution identified by the optimization algorithm fulfills the constraints in all points except for $k = 48$. This point coincides with the unique time step at which outdoor temperature $T_o$ is greater than the indoor temperature $T_a$, as shown in figure 7b. The outdoor temperature increase won't influence the indoor temperature until the next time step. According to equation 6, at this point the air flow becomes zero because of the *max* function evaluation and can not be influenced by $u(k)$. The value of $u$ at $k = 48$ is let by the optimization algorithm at the value provided in the initial conditions.

Further attempts to improve the solution such that the constraints are met in all points were not successful. Therefore, it is concluded that finding a solution in the feasible set is not possible in the given context and the mass flow rate can meet the constraint in the first 4 hours ($k < 48$).

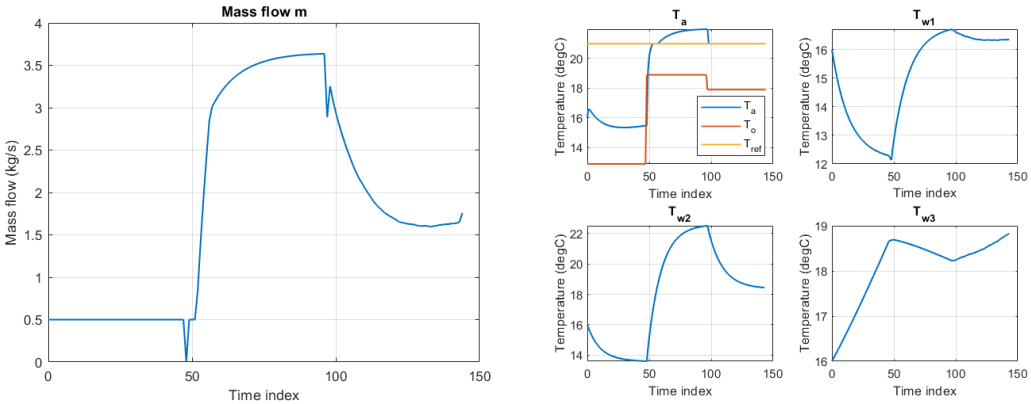


(a) Constrained air flow

(b) Evolution of states

Figure 7: System evolution with air mass flow constraint

# 8 Unconstrained airflow, constrained airflow and no control cases comparison

Figure 8a illustrates a comparison between values of fraction $u$. Both solutions obtained by minimization have the same value at $k = 48$, due to the zero value of the air mass flow. There are visible (but

not considerable) differences between the solutions of the optimization problems in both $u$ and $v$ after time instant $k = 98$. In the no control case, $u$ and $v$ are constant and equal to 1 along the time interval.

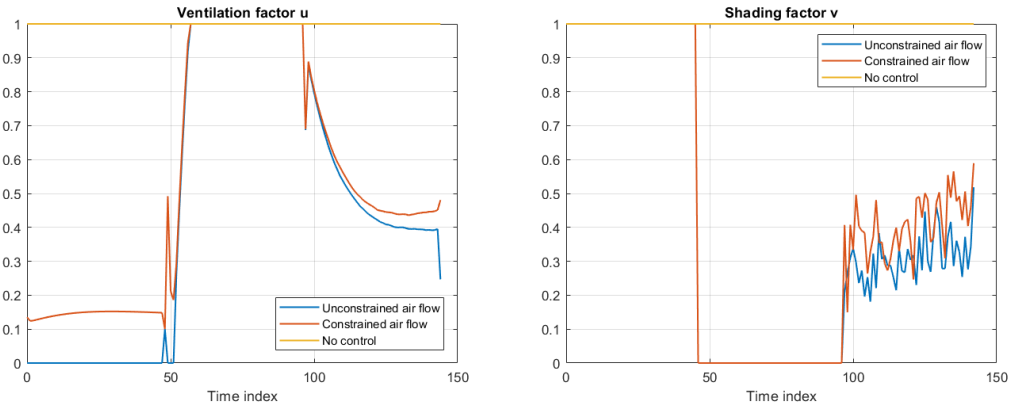


(a) Ventilation factor $u$

(b) Shading factor $v$

Figure 8: Comparison of dynamic values of $u(k)$ and $v(k)$

The energy demand in the no control case is considerably larger than that of the optimized cases over the entire time horizon (figure 9). This is a consequence of fractions $u$ and $v$ not being adapted to environment factors (air mass flow in the thermal tower and solar radiation are not limited). In addition, $q_{backup}$ is larger when the air flow is constrained to be greater than 0.5 kg/s than when it is unconstrained because the system demands more energy to keep the air flow at the desired value. These observations are reflected in the minimal backup demand for the three cases, shown in table 2.

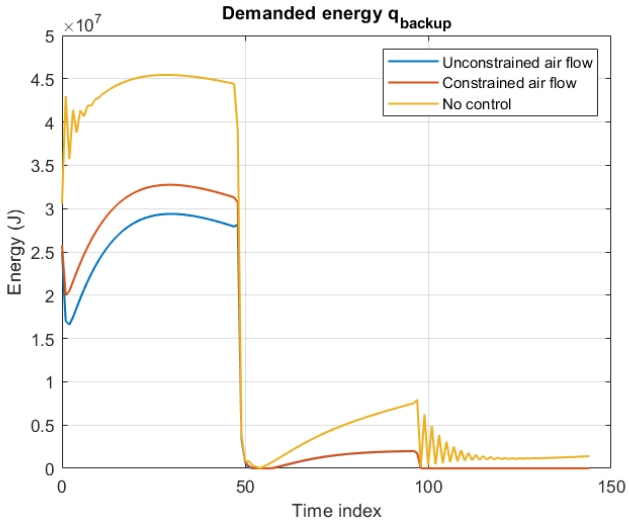


Figure 9: Comparison of energy demand for the three cases

| | Energy demand (J) |
|---|---|
| Unconstrained $\dot{m}$ | 1.3638e+09 |
| Constrained $\dot{m}$ | 1.5347e+09 |
| No control | 2.4077e+09 |

Table 2: Minimal backup energy demand

# References

[vdBS21] Ton van den Boom and Bart De Schutter. Lecture Notes for the Course SC42056, September 2021.